Tetrahedron Letters 51 (2010) 5185–5190

Contents lists available at ScienceDirect

Tetrahedron Letters

journal homepage: www.elsevier.com/locate/tetlet

A general equation correlating intramolecular rates with 'attack' parameters: distance and angle

Rafik Karaman *

Faculty of Pharmacy, Al-Quds University, PO Box 20002, Jerusalem, Palestine

ARTICLE INFO

Article history:
Received 1 June 2010
Revised 14 July 2010
Accepted 23 July 2010
Available online 3 August 2010

Keywords:
Intramolecularity
Proton transfer reactions
Enzyme catalysis
DFT calculations
Proximity orientation

ABSTRACT

Using density functional theory (DFT) at the B3LYP level with the 6-31G(d,p) basis set, a general equation is derived relating activation energy with the distance between the two reactive centers (r_{GM}), and the hydrogen-bonding angle (α_{GM}) in an intramolecular proton transfer process. The strong correlation between the values of r_{GM} and α_{GM} with the activation energy, $\Delta G^{\ddagger}$, which reflects the experimental reaction rate, provides an excellent tool to predict reaction rate based on calculated geometrical parameters for a certain system ($\Delta H^{\ddagger}$, $\Delta G^{\ddagger}$ vs r_{GM} and α_{GM}). The slope of the equation can be used as an indicator of the mode by which the two reacting centers orchestrate in an intramolecular process.

The chemistry of intramolecular processes has been important in modeling the extraordinary efficiency of enzymes. Both are similar in that the reacting centers and are held together (covalently with intramolecular systems, and non-covalently with enzymes).[1] Although Menger, in his spatiotemporal theory, invoked the distance between reactants as a key element of reactivity,[2] an idea later expanded by Bruice in his related 'near attack conformation' concept,[3] the notion of 'proximity' has never been quantified adequately. Despite decades of attention on intramolecularity, the details of how intramolecular rates depend on distance/angle relationships between a nucleophile and an electrophile remain unclear. In this Letter, geometric aspects of intramolecular reactivity are addressed including the derivation of an equation that strongly correlates reaction rate with distance/angle for 18 intramolecular proton transfer processes.

Recently, we have investigated the mechanistic pathways for some intramolecular processes that have been utilized as enzyme models. Exploiting ab initio and DFT theoretical calculation methods, we have explored: (a) acid-catalyzed lactonization of hydroxyacids as studied by Cohen[4] and Menger;[2] (b) S_N2-based cyclization as researched by Brown, Bruice, and Mandolini;[3,5] (c) proton transfer in rigid tricarboxylic amides as investigated by Menger;[2] and (d) addition of nucleophiles to a C=C double bond as explored by Kirby,[6] and arrived at the following conclusions: (1) the driving force for rate enhancement in intramolecular processes can be due to proximity and/or steric effects, depending on the nature of the system, and the accelerations in rate for intramolecular reactions are a result of both entropic and enthalpic effects. (2) In S_N2-based ring-closing reactions leading to three-, four- and five-membered rings the *gem*-dialkyl effect is more dominant in those involving formation of an unstrained five-membered ring, and the need for directional flexibility decreases on increasing the size of the ring being formed. In addition, the demands on directional flexibility decrease on increasing the volume of the nucleophile involved in the S_N2 ring-closing reaction. Furthermore, it has been concluded from these studies that understanding the mechanisms by which systems execute their reactions is a stepping stone for the design of chemical entities (prodrugs) that might have the ability to undergo cleavage reactions in physiological environments at rates that are completely dependent on the structural features of the host (inactive linker).[7]

In this Letter, DFT quantum molecular orbital investigations of ground state and transition state structures, vibrational frequencies, and reaction trajectories for the intramolecular proton transfer reactions in processes **1**–**18** are described.

The aims of this study were to: (a) unravel the nature of the driving force(s) affecting the efficiency of the proton transfer in the three different systems described in Schemes 1a and b, and (b) establish a correlation between proton transfer rate and the 'attack' parameters, that is, the distance between the two reacting centers and the hydrogen-bonding angle.

Computational efforts were directed toward elucidation of the transition and ground state structures for the proton transfer processes in **1**–**18** due to the importance of intramolecular hydrogen bonding on the stability of the ground states, the derived transition states, and consequently, the corresponding products.[8]

* Tel.: +972 2 548132234; fax: +972 2 2790413.
E-mail address: dr_karaman@yahoo.com

0040-4039/$ - see front matter © 2010 Elsevier Ltd. All rights reserved.
doi:10.1016/j.tetlet.2010.07.137

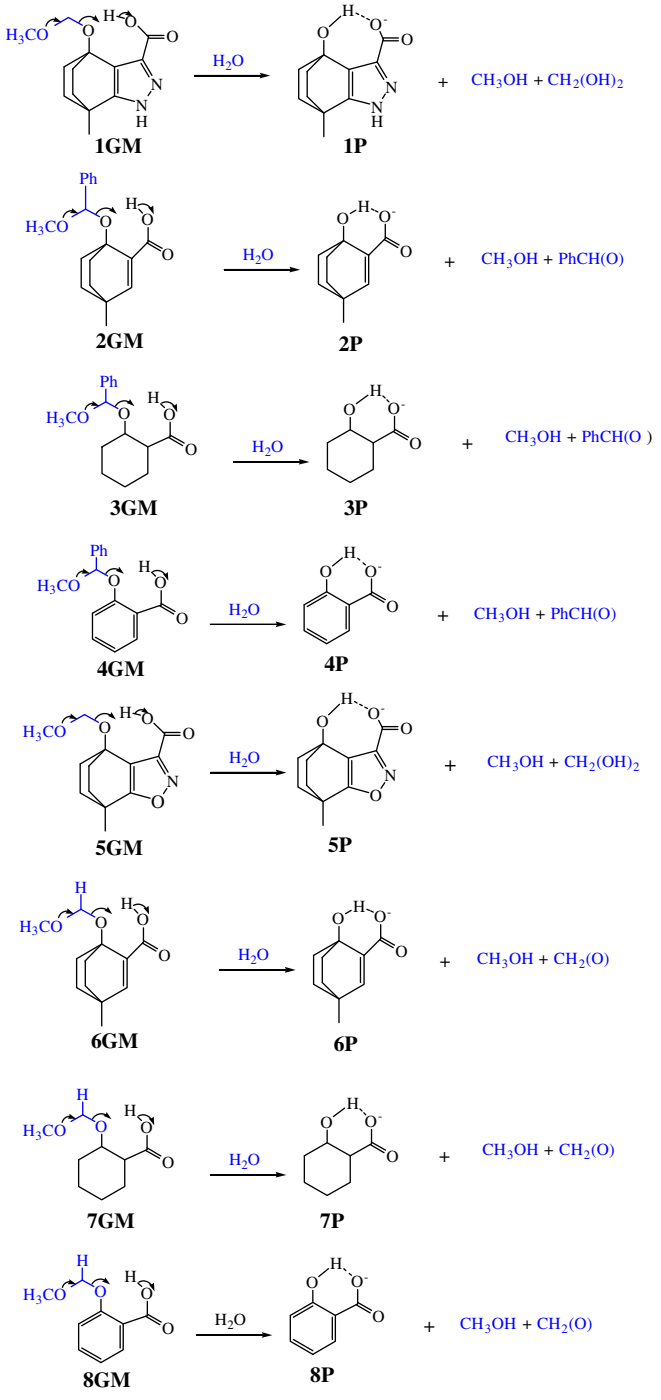

Scheme 1a. Intramolecular proton transfer reactions in **1–8**, where GM and P are the reactants and products, respectively.

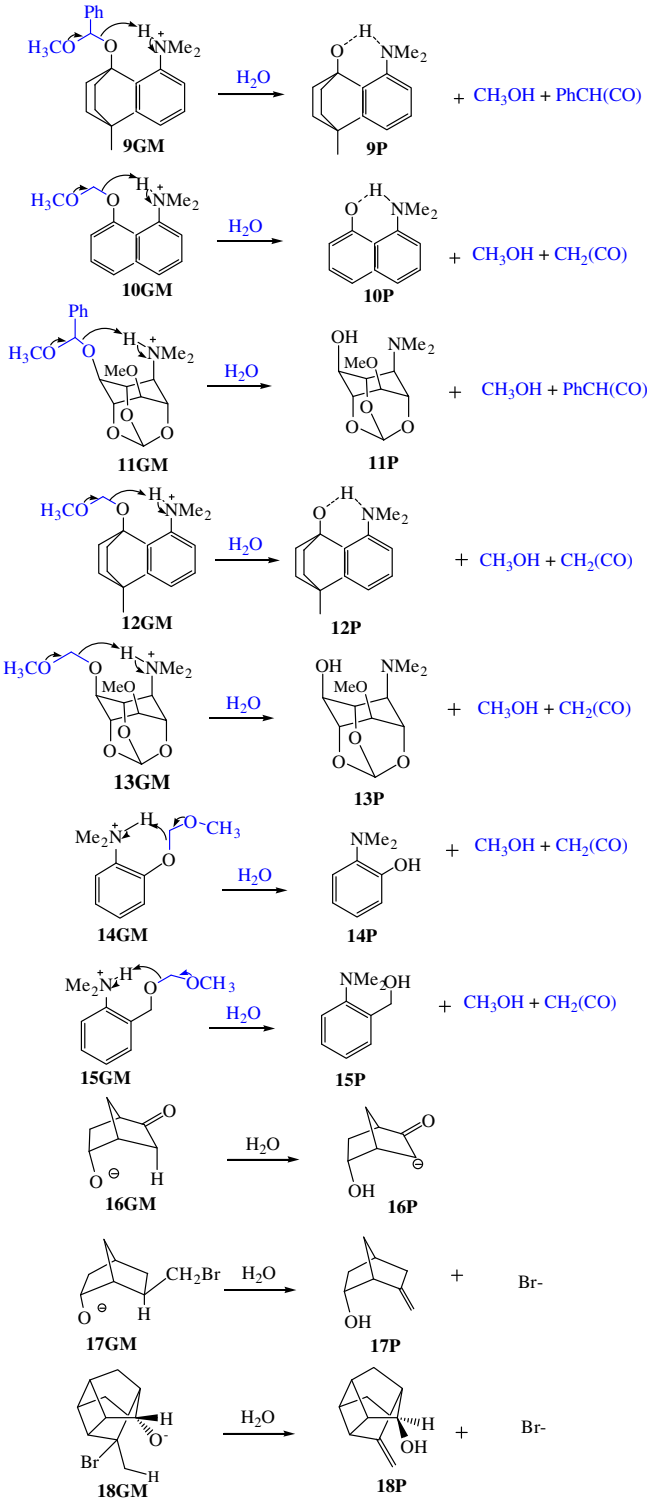

Scheme 1b. Intramolecular proton transfer reactions in **9–18**, where GM and P are the reactants and products, respectively.

The three intramolecular proton transfer reactions shown in Schemes 1a and b, and cited here to illustrate the general utility of the rate/geometry relationship are: (a) proton transfer between two oxygens in Kirby's acetals;[8] (b) proton transfer between nitrogen and oxygen in Kirby's enzyme models,[8] and (c) proton transfer between carbon and oxygen in rigid systems as studied by Menger.[2]

Using the DFT molecular orbital method, the ground and transition state properties of the intramolecular proton transfer in which compounds **1–18** are engaged were calculated (see calculation methods, Supplementary data).[9] Utilizing the calculated DFT enthalpic and entropic energies for the global minima (GM) of **1–18** and the derived transition states structures (TS) (*Table* S1, Supplementary data) the enthalpic activation energies ($\Delta H^{\ddagger}$), the entropic activation energies ($T\Delta S^{\ddagger}$), and the free activation energies ($\Delta G^{\ddagger}$) for the corresponding proton transfer reactions have been calculated. The calculated data are summarized in Table 1 and include the calculated DFT distance between the two reacting centers in the ground state (r_{GM}) and in the transition state (r_{TS}), as well as the calculated DFT hydrogen-bonding angles α_{GM} and α_{TS} as defined in Figure 1.

Table 1
DFT (B3LYP/6-31G (d,p))-calculated kinetic and thermodynamic properties for the proton transfers in **1**–**18**

System	X–H···O	r_{GM} (Å)	r_{TS} (Å)	α_{GM} (°)	β_{TS} (°)	$\Delta H^{\ddagger}$	$T\Delta S^{\ddagger}$	$\Delta G^{\ddagger}$
1	O–H···O	1.70	1.37	170	170	27.78	−2.68	30.46
2	O–H···O	1.69	1.37	149	144	31.38	−3.71	35.09
3	O–H···O	3.66	1.37	48	131	41.09	1.04	40.05
4	O–H···O	1.74	1.37	147	153	29.04	−5.12	34.16
5	O–H···O	1.72	1.37	171	162	29.30	0.03	29.27
6	O–H···O	1.69	1.37	143	143	33.09	−1.25	34.34
7	O–H···O	3.60	1.37	14	131	44.29	−2.23	46.52
8	O–H···O	1.96	1.37	147	150	34.32	−3.42	37.74
9	N–H···O	1.72	1.54	146	140	23.62	0.07	23.55
10	N–H···O	2.04	1.54	125	125	24.73	−3.34	28.07
11	N–H···O	3.33	1.54	123	–	25.41	−4.15	29.56
12	N–H···O	1.73	1.54	144	145	22.54	0.90	21.64
13	N–H···O	3.33	1.54	124	–	23.59	−4.15	27.74
14	N–H···O	1.92	1.54	122	122	29.33	0.61	28.72
15	N–H···O	2.51	1.54	107	133	34.71	−2.00	36.71
16	C–H···O	2.25	1.54	109	137	11.87	−0.25	12.12
17	C–H···O	2.26	1.54	112	131	7.16	0.48	6.68
18	C–H···O	1.73	1.54	153	149	0.00	−0.57	0.57

r_{GM} and r_{TS} are the distances between the two reactive centers in the ground and transition states, respectively (Fig. 1). $\Delta H^{\ddagger}$ is the activation enthalpic energy (kcal/mol). $T\Delta S^{\ddagger}$ is the activation entropic energy in kcal/mol. $\Delta G^{\ddagger}$ is the activation free energy (kcal/mol). α_{GM} is the hydrogen-bonding angle in the ground state structure (Fig. 1). α_{TS} is the hydrogen-bonding angle in the transition state structure (Fig. 1).

Figure 2a and b and S1 (Supplementary data) show the DFT-calculated global minimum (GM) and transition state (TS) structures for **1**–**18** (Schemes 1a and b). Inspection of the GM structures for the proton transfer reaction occurring between the carboxyl hydroxy group and the β or γ ether oxygen in processes **1**, **2**, **4–6**, and **8** (**1GM–2GM**, **4GM–6GM**, and **8GM**) reveals that the two moieties are engaged, intramolecularly, in hydrogen bonding whereas the interaction with the solvent (water) molecules is via the other ether oxygen (Fig. 2 and S1a). This engagement results in the formation of seven-membered rings for **1GM** and **5GM** and six-membered rings for **2GM–4GM** and **6GM–8GM** (Fig. 1a and Sa1). Further, the DFT-calculated hydrogen-bonding length (r_{GM}) for **1GM–2GM, 4GM–6GM**, and **8GM** was found in the range of 1.69–1.96 Å and the attack angle α (the hydrogen-bond angle, α_{GM}) was in the range of 143–171° (Table 1). On the other hand, the GM structures in processes **3** and **7** (**3GM** and **7GM**) were found to participate in intermolecular hydrogen bonding with a molecule of water rather than in an intramolecular manner. This is due to the fact that the r_{GM} value in both structures is relatively long (Fig. S1a). Thus, the preference for intermolecular over intramolecular engagement might be attributed to the high energy barrier for rotation of the carboxyl group around the cyclohexyl moiety.[10]

Similarly, inspection of the GM structures, **9GM–15GM**, for the proton transfer reaction from nitrogen to the β or γ ether oxygen in **9–15**, revealed that all of the geometries, except **11GM** and **13GM**, exhibited a conformation in which the ammonium group forms a hydrogen bond with the neighboring alkoxy oxygen. This

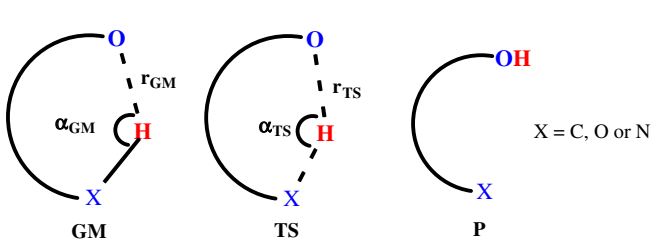

Figure 1. Representation of an energy profile describing an intramolecular process. r_{GM} is the distance between the two reactive centers and α_{GM} and α_{TS} are the hydrogen-bonding angles in the global minimum (GM) and transition state (TS) structures, respectively. P is the product.

engagement results in the formation of six-membered rings for **9GM–10GM**, **12GM**, and **14GM**, and a five-membered ring for **15GM** (Fig. 2a and S1a). The DFT-calculated r_{GM} values for **9GM–10GM, 12GM**, and **14GM–15GM** were in the range 1.72–2.51 Å and the attack angle α (the hydrogen-bond angle, α_{GM}) was in the range 107–146°. On the other hand, no intramolecular hydrogen bonding occurred in the GM structures of **11** and **13** (**11GM** and **13 GM**). The distance, r_{GM}, between the ammonium proton and the ether oxygen in **11GM** and **13 GM** was 3.33 Å (Fig. S1a and Table 1). The GM structures for **11** and **13** were found to interact in an intermolecular fashion with a water molecule where the latter hydrogen bonds with both the ammonium and the ether groups.

Examination of the optimized global minimum structures, **16GM–18GM**, in processes **16–18** where a proton is transferred from a carbon to an oxygen indicates that the three structures are engaged in intramolecular hydrogen bonding. This engagement furnishes five-membered rings for **16GM** and **17GM** and a six-membered ring for **18GM** (see Fig. 2a and S1a). The calculated r_{GM} values for **16GM–18GM** were in the range 1.73–2.26 Å and the attack angle α (the hydrogen-bond angle, O···H–O) was in the range 109–153° (Table 1).

Furthermore, Table 1 indicates that the distance between the two reactive centers (r_{GM}) varies according to the conformation in which the GM resides. A short r_{GM} distance is achieved when the value of the hydrogen-bonding angle (α_{GM}) is high and close to 180°, whereas α_{GM} values far removed from 180° were obtained when the r_{GM} distance was relatively long. When the r_{GM} and α_{GM}-calculated DFT values listed in Table 1 were examined for linear correlation a strong correlation was obtained with a correlation coefficient of $R = 0.96$ (Fig. 3a). In addition, Table 1 shows that the free activation energy ($\Delta G^{\ddagger}$) needed to execute a proton transfer in the three systems, **1–8**, **9–15**, and **16–18**, was largely dependent on both the distance between the two reactive centers, r_{GM}, and the hydrogen-bonding angle, α_{GM}. Systems having GM structures that exhibit short r_{GM} and high α_{GM} values (close to 180°) such as **1** and **5**, **9** and **12**, and **18** are characterized with higher rates (lower $\Delta G^{\ddagger}$) than those having long r_{GM} and low α_{GM} values, such as **3** and **7**, **15**, and **16**. Linear correlation of the calculated DFT enthalpic energies ($\Delta H^{\ddagger}$) with r_{GM} values gave good correlations with correlation coefficients (R) of 0.93 for systems **1–8**, 0.90 for **9–15**, and 0.91 for **16–18**. Furthermore, the calculated enthalpic ($\Delta H^{\ddagger}$) and free activation ($\Delta G^{\ddagger}$) energies were found to correlate very well with $r_{GM}^2 \times \sin(180 - \alpha_{GM})$. The correlation coefficients (R) for the correlations with $\Delta H^{\ddagger}$ are 0.98 for **1–8**, 0.92 for **9–15**, and 0.92 for **16–18** (Fig. 3b), and those with $\Delta G^{\ddagger}$ are 0.95 for **1–8**, 0.89 for **9–15**, and 0.98 for **16–18** (Fig. 3c).

Comparison of the slopes for the three curves illustrated in Figure 3b and c reveals that **16–18** have the highest slope whereas **1–8** have the lowest. Furthermore, it was found that the order of the slope values (S) for $\Delta H^{\ddagger}$ and $\Delta G^{\ddagger}$ versus $r_{GM}^2 \times \sin(180 - \alpha_{GM})$ in systems **1–18** was: $S_{\mathbf{16–18}} > S_{\mathbf{9–15}} > S_{\mathbf{1–8}}$, and when the S values were plotted against r_{TS} values, very strong correlations were obtained (Fig. 3d). This result indicates an early transition state for the proton transfer between two oxygens (systems **1–8**) and a relatively late transition state for transfer of a proton from nitrogen to oxygen (systems **9–15**) and from carbon to oxygen (systems **16–18**).

In order to explore in depth the mode and action of the proton transfer in the systems studied, the values of $(\alpha_{TS} - \alpha_{GM})$ were examined for linear correlation with the enthalpic ($\Delta H^{\ddagger}$) and the free activation energies ($\Delta G^{\ddagger}$). The correlation results indicate a relatively good correlation with correlation coefficients of $R = 0.86–0.99$. Proton transfer for systems having low $(\alpha_{TS} - \alpha_{GM})$ values were faster than those having higher $(\alpha_{TS} - \alpha_{GM})$ values. For example, the $(\alpha_{TS} - \alpha_{GM})$ value for process **1** is 0 and its activation energy is 30.46 kcal/mol, whereas for process **7** the $(\alpha_{TS} - \alpha_{GM})$

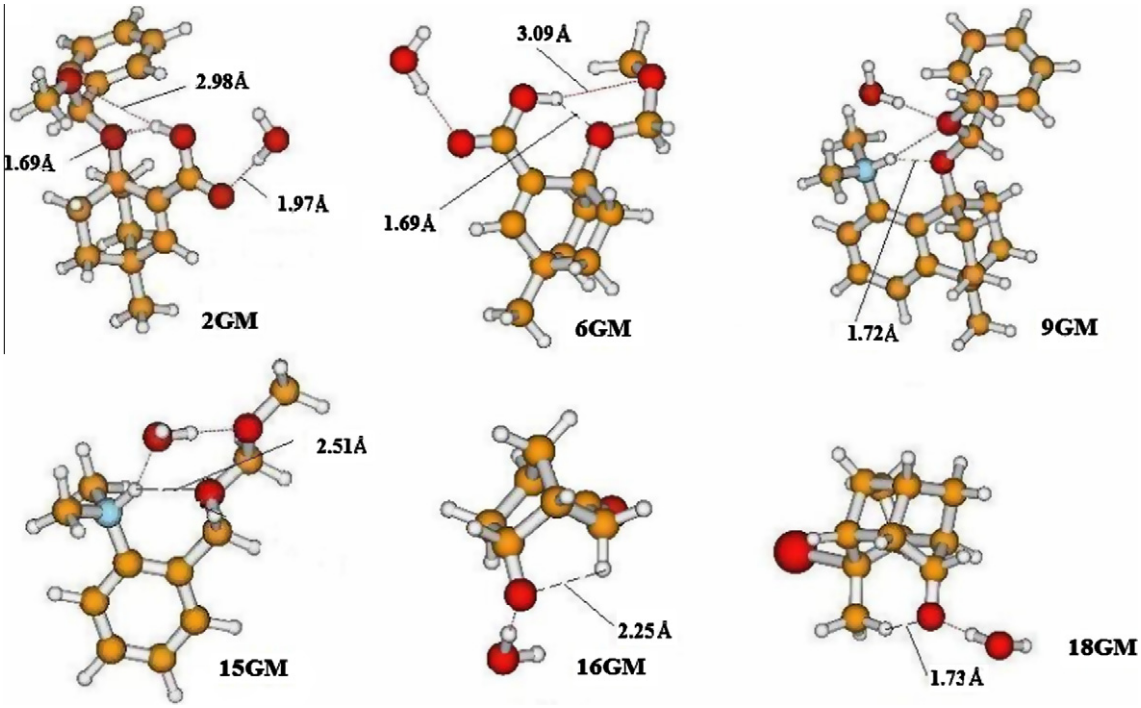

Figure 2a. DFT-optimized global minimum (GM) structures in the intramolecular proton transfer reactions of **2**, **6**, **9**, **15**, **16**, and **18**.

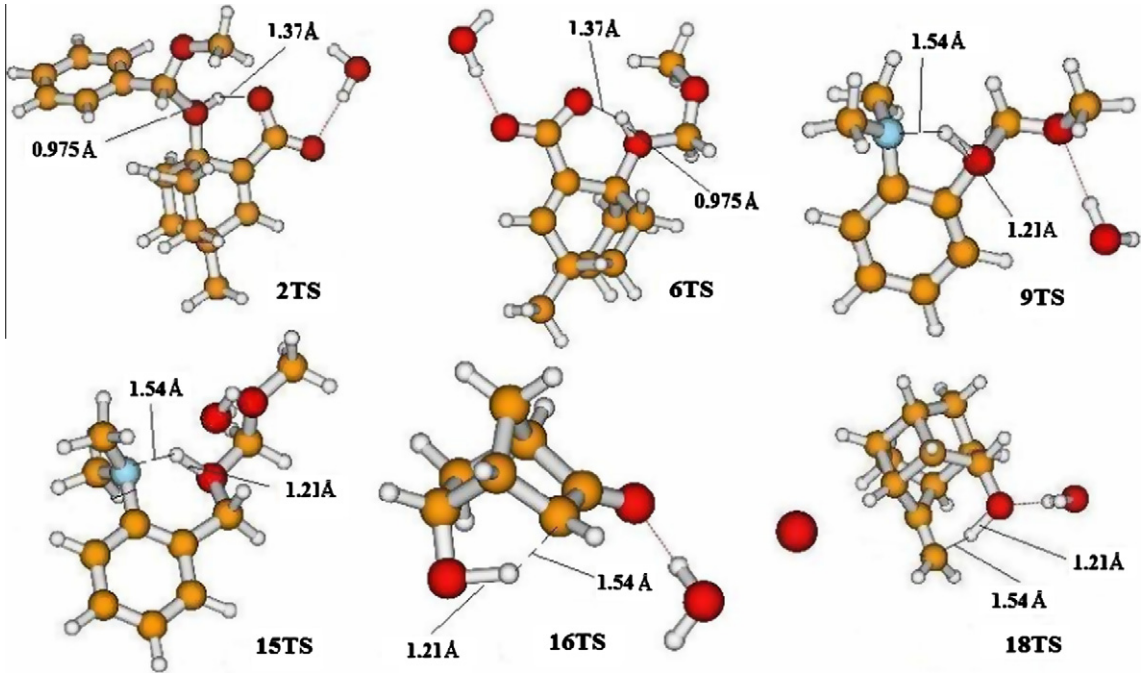

Figure 2b. DFT-optimized transition state (TS) structures in the intramolecular proton transfer reactions of **2**, **6**, **9**, **15**, **16**, and **18**.

value is 117 and its $\Delta G^{\ddagger}$ is 46.52 kcal/mol (Table 1). This is intuitively feasible as one would expect that a low energy barrier is needed when the structures of the starting geometry and the transition state are quite similar.

In summary, we have introduced a general equation that relates activation energy to hydrogen-bonding angle and distance between the two reactive centers. The strong correlation between the values of the calculated $\Delta G^{\ddagger}$, which reflects the experimental reaction rate, and geometrical parameters provides an excellent tool to predict reaction rate based on a calculated GM for a certain system [$\Delta G^{\ddagger}$ vs $r^2_{GM} \times \sin(180 - \alpha_{GM})$]. The slope of the equation (S) can be used as an indicator of the mode by which the two reacting centers are orchestrated in an intramolecular process.

Careful examination of the correlation equation depicted in Figure 3c reveals that the term $\sin(180 - \alpha_{GM})$ is decreased in systems having a relatively linear hydrogen bond between the proton and the two acceptors that results in reduced activation energy. Therefore, the proton transfer rate in an intramolecular process is

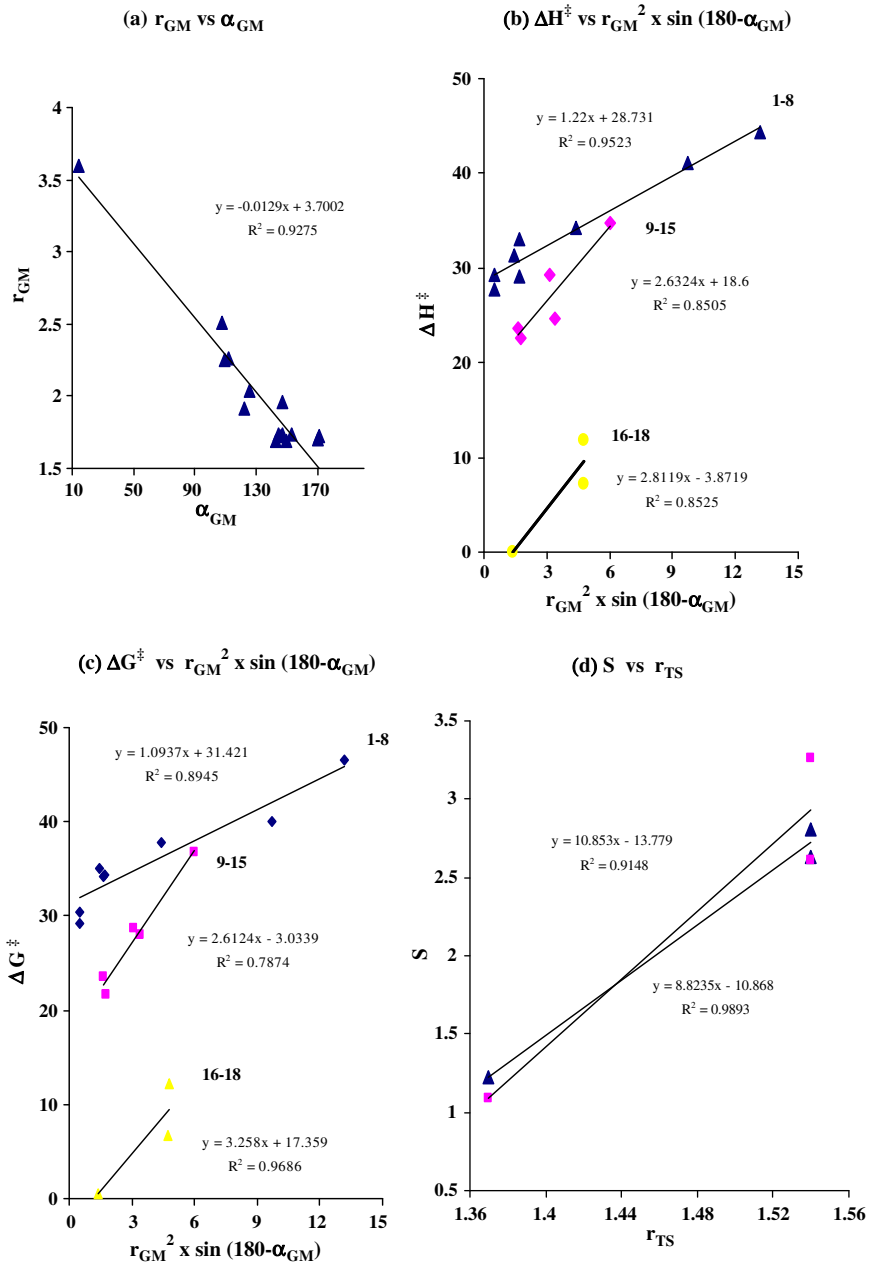

Figure 3. (a) Plot of the DFT-calculated r_{GM} versus α_{GM} in **1**–**18**, where r_{GM} is the distance between the two reactive centers and α_{GM} is the hydrogen-bonding angle. (b) Plot of the DFT-calculated $\Delta H^{\ddagger}$ versus $r_{GM}^2 \times \sin(180 - \alpha_{GM})$ in **1**–**18**, where α_{GM} is the attack angle and r_{GM} is the distance between the two reactive centers in the GM structure. (c) Plot of the DFT-calculated $\Delta G^{\ddagger}$ versus $r_{GM}^2 \times \sin(180 - \alpha_{GM})$ in **1**–**18**, where α_{GM} is the attack angle and r_{GM} is the distance between the two reactive centers in the GM structure. (d) Plot of the slope (S) versus r_{TS} where S is the slope of $\Delta G^{\ddagger}$ versus $r_{GM}^2 \times \sin(180 - \alpha_{GM})$ for **1**–**18** and r_{TS} is the distance between the hydrogen and the heteroatom.

determined based on the linearity of the hydrogen bonding in the reactant and the greater the deviation from linearity the lower is the rate.

The DFT calculation results have revealed that the proton transfer rate in systems **1**–**18** is quite responsive to geometric disposition, especially in relation to the distance between the two reactive centers, r_{GM}, and the angle of attack, α_{GM}. Requirements for a system to achieve a high intramolecular proton transfer rate are: (1) a short distance between the two reactive centers (r_{GM}) in the ground state which subsequently results in a strong intramolecular hydrogen bonding, and (2) the difference between the hydrogen-bonding angle α_{GM} in the ground state and the angle α_{TS} formed in the transition state should be minimal. This maximizes the orbital overlap of the two reactive centers when they are engaged along the reaction pathway.

To lend more credibility to the DFT calculation results, the DFT-calculated log EM values for processes **1**, **2**, and **9** (10.58, 5.21 and 3.07, respectively) were examined for correlation with the experimental values (10 for **1**, 3.48 for **2**, and 4 for **9**). A linear correlation with a coefficient of 0.94 was obtained.[8]

It is tempting to extrapolate our results to enzymes. Accordingly, we propose that enzymes achieve their remarkable catalytic activity by imposing a range of contact distances within the space of hydrophobic pockets at the active site.[1] These contact distances and space can be varied according to the nature of the enzyme. For enzymes that are involved in catalysis of proton transfer processes, such as chymotrypsin, the distance and the space are fit such that a proton (an electrophile) can approach a nucleophile more easily when a strong hydrogen bond is formed in the transition state, and subsequently in their corresponding products. This proposal

expresses the notion of Menger's spatiotemporal control and Kirby's explanation of an efficient proton transfer in enzyme-catalyzed reactions.[2,8]

Acknowledgments

Karaman Co. is thanked for support of our computational facilities. Special thanks are given to Angi Karaman, Donia Karaman, Rowan Karaman, and Nardene Karaman for technical assistance.

Supplementary data

Supplementary data (Table S1, DFT calculated properties for **1GM**-**18GM** and **1TS**-**18TS**; Fig. S1, DFT optimized global minimum and transition state structures in processes **1**–**18**; calculation methods, xyz cartesian coordinates for the calculated GM and TS optimized structures in processes **1**–**18**) associated with this article can be found, in the online version, at doi:10.1016/j.tetlet.2010.07.137.

References and notes

1. (a) Hanson, K. R.; Havir, E. A., 3rd ed.. In *The Enzymes*; Boyer, P. D., Ed.; Academic Press: New York, 1972; Vol. 7, p 75; (b) Williams, V. R.; Hiroms, J. M. *Biochem. Biophys. Acta* **1967**, *139*, 214; (c) Klee, C. B.; Kirk, K. L.; Cohen, L. A.; McPhie, P. *J. Biol. Chem.* **1975**, *250*, 5033; (d) Hanson, K. R.; Havir, E. A. *Biochemistry* **1968**, *7*, 1904; (e) Czarin, A. W. In *Mechanistic Principles of Enzyme Activity*; Liebman, J. F., Greenberg, A., Eds.; VCH: New York, 1988; (f) Nelson, D. L.; Cox, M. M. *Lehninger Principles of Biochemistry*; Worth: New York, 2003; (g) Fersht, A. *Structure and Mechanism in Protein Science. A guide to Enzyme Catalysis and Protein Folding*; Freeman, W. H. and Company: New York, 1999; (h) Pascal, R. *Eur. J. Org. Chem.* **2003**, 1813; (i) Pascal, R. *Bioorg. Chem.* **2003**, *31*, 485; (j) Page, M. I.; Jencks, W. P. *Gazz. Chim. Ital.* **1987**, *117*, 455; (k) Sweigers, G. F. *Mechanical Catalysis*; John Wiley & Sons: Hoboken, NJ, 2008; (l) Walsh, C. *Enzymatic Reaction Mechanisms*; San Francisco: Freeman, 1979. p 978.
2. (a) Menger, F. M. *Acc. Chem. Res.* **1985**, *18*, 128; (b) Menger, F. M.; Chow, J. F.; Kaiserman, H.; Vasquez, P. C. *J. Am. Chem. Soc.* **1983**, *105*, 4996; (c) Menger, F. M. *Tetrahedron* **1983**, *39*, 1013; (d) Menger, F. M.; Grossman, J.; Liotta, D. C. *J. Org. Chem.* **1983**, *48*, 905; (e) Menger, F. M.; Galloway, A. L.; Musaev, D. G. *Chem. Commun.* **2003**, 2370; (f) Menger, F. M. *Pure Appl. Chem.* **2005**, *77*, 1873. and references cited therein.
3. (a) Bruice, T. C.; Lightstone, F. L. *Acc. Chem. Res.* **1999**, *32*, 127; (b) Lightstone, F. L.; Bruice, T. C. *J. Am. Chem. Soc.* **1997**, *119*, 9103; (c) Lightstone, F. L.; Bruice, T. C. *J. Am. Chem. Soc.* **1996**, *118*, 2595; (d) Lightstone, F. L.; Bruice, T. C. *J. Am. Chem. Soc.* **1994**, *116*, 10789; (e) Bruice, T. C.; Bradbury, W. C. *J. Am. Chem. Soc.* **1968**, *90*, 3803; (f) Bruice, T. C.; Bradbury, W. C. *J. Am. Chem. Soc.* **1965**, *87*, 4846; (g) Bruice, T. C.; Pandit, U. K. *J. Am. Chem. Soc.* **1960**, *82*, 5858; (h) Bruice, T. C.; Pandit, U. K. *Proc. Natl. Acad. Sci. U.S.A.* **1960**, *46*, 402.
4. (a) Milstein, S.; Cohen, L. A. *J. Am. Chem. Soc.* **1970**, *92*, 4377; (b) Milstein, S.; Cohen, L. A. *Proc. Natl. Acad. Sci. U.S.A.* **1970**, *67*, 1143; (c) Milstein, S.; Cohen, L. A. *J. Am. Chem. Soc.* **1972**, *94*, 9158; (d) Borchardt, R. T.; Cohen, L. A. *J. Am. Chem. Soc.* **1972**, *94*, 9166; (e) Borchardt, R. T.; Cohen, L. A. *J. Am. Chem. Soc.* **1972**, *94*, 9175; (f) Borchardt, R. T.; Cohen, L. A. *J. Am. Chem. Soc.* **1973**, *95*, 8308; (g) Borchardt, R. T.; Cohen, L. A. *J. Am. Chem. Soc.* **1973**, *95*, 8313; (h) King, M. M.; Cohen, L. A. *J. Am. Chem. Soc.* **1983**, *105*, 2752; (i) Hillery, P. S.; Cohen, L. A. *J. Org. Chem.* **1983**, *48*, 3465.
5. (a) Brown, R. F.; Van Gulick, N. M. *J. Org. Chem.* **1956**, *21*, 1046; (b) Galli, C.; Mandolini, L. *Eur. J. Org. Chem.* **2000**, 3117.
6. (a) Bada, J. L.; Miller, S. L. *J. Am. Chem. Soc.* **1970**, *92*, 2744; (b) Kirby, A. J.; Logan, C. J. *J. Chem. Soc., Perkin Trans. 2* **1977**, 642.
7. (a) Karaman, R. *Bioorg. Chem.* **2009**, *37*, 11; (b) Karaman, R. *Tetrahedron Lett.* **2008**, *49*, 5998; (c) Karaman, R. *Tetrahedron Lett.* **2009**, *50*, 452; (d) Karaman, R. *Res. Lett. Org. Chem.* doi:10.1155/2009/240253.; (e) Karaman, R. *Bioorg. Chem.* **2009**, *37*, 106; (f) Karaman, R. *J. Mol. Struct. (Theochem)* **2009**, *910*, 27; (g) Karaman, R. *Tetrahedron Lett.* **2009**, *50*, 6083; (h) Karaman, R. *J. Mol. Struct. (Theochem)* **2010**, *939*, 69; (i) Karaman, R. *Tetrahedron Lett.* **2009**, *50*, 7304; (j) Karaman, R. *J. Mol. Struct. (Theochem)* **2010**, *940*, 70; (k) Karaman, R. *Tetrahedron Lett.* **2010**, *51*, 2130; (l) Karaman, R. *J. Mol. Phys.* **2010**, *108*, 1723; (m) Karaman, R. *Int. Rev. Biophys. Chem.*, in press.
8. (a) Kirby, A. J. *Acc. Chem. Res.* **1997**, *30*, 290; (b) Kirby, A. J.; Parkinson, A. *J. Chem. Soc., Chem. Commun.* **1994**, 707; (c) Brown, C. J.; Kirby, A. J. *J. Chem. Soc., Perkin Trans. 2* **1997**, 1081; (d) Craze, G.-A.; Kirby, A. J. *J. Chem. Soc., Perkin Trans. 2* **1978**, 354; (e) Craze, G.-A.; Kirby, A. J.; Osborne, R. *J. Chem. Soc., Perkin Trans. 2* **1978**, 357; (f) Craze, G.-A.; Kirby, A. J. *J. Chem. Soc., Perkin Trans. 2* **1974**, 61; (g) Barber, S. E.; Dean, K. E. S.; Kirby, A. J. *Can. J. Chem.* **1999**, 792; (h) Asaad, N.; Davies, J. E.; Hodgson, D. R. W.; Kirby, A. J. *J. Phys. Org. Chem.* **2005**, *18*, 101; (i) Kirby, A. J.; Lima, M. F.; de Silva, D.; Roussev, C. D.; Nome, F. *J. Am. Chem. Soc.* **2006**, *128*, 16944; (j) Kirby, A. J.; Williams, N. H. *J. Chem. Soc., Perkin Trans. 2* **1994**, 643; (k) Kirby, A. J.; Williams, N. H. *J. Chem. Soc., Chem. Commun.* **1991**, 1643; (l) Hartwell, E.; Hodgson, D. R. W.; Kirby, A. J. *J. Am. Chem. Soc.* **2000**, *122*, 9326.
9. For details of the calculation methods, see: Supplementary data. http://www.gaussian.com.
10. An energy of 5 kcal/mol was needed to rotate the carboxyl group such that the hydrogen bonding angle increases from 48° to 88°. Fife, T. H.; Przystas, T. J. *J. Am. Chem. Soc.* **1979**, *101*, 1202.